

Josephson superlattices and low-amplitude gap solitons

D. Barday and M. Remoissenet

Laboratoire Ondes et Structures Cohérentes (OSC), Faculté des Sciences et Techniques, Université de Bourgogne, 6 boulevard Gabriel, 21100 Dijon, France

(Received 27 December 1989)

We have examined the amplitude dependence of the transmission properties in the natural gap of a finite Josephson transmission line and in the first artificial gap of a finite Josephson superlattice. We show that the nonlinear transmission response of both systems exhibits gap-soliton-mediated bistability and hysteresis and can approach unity, once the amplitude of the incoming wave is greater than a certain threshold which is frequency dependent and also decreases with the length of the system. Our computer experiments on the dynamics of wave transmission, which show how the systems would behave in practice, are in good agreement with our calculations and the theoretical predictions in the literature for other kinds of superlattices. We have observed that the modulational instability in the Benjamin-Feir sense which may appear in some computer experiments is eliminated if one considers weak dissipative systems.

I. INTRODUCTION

The superconducting Josephson transmission line¹⁻⁵ has proven to be one of the most successful testing grounds for nonlinear wave theory. It is a physical system where soliton properties are most accessible for direct experimental investigations. Furthermore, the use of Josephson transmission lines (JTL) for information processing and storage is quite attractive, and one expects more interesting applications in the near future in light of the recent discoveries of the new high- T_c superconductors.

On the other hand, the nonlinear properties of superlattices are fascinating, because such periodic structures exhibit a rich variety of collective properties not shared by their constituents. One interesting example is provided in optics by the propagation of electromagnetic radiation through multilayer structures, normal to the interfaces. In the linear regime, the propagation of waves through the superlattice is described by a dispersive relation which contains gaps also called stop gaps. The envelope of any wave whose frequency lies in a stop gap or forbidden band undergoes an exponential decay with distance down the structure, and the transmissivity of a superlattice of finite length is exponentially small. In the nonlinear regime, where the refractive index depends on the field intensity (Kerr effect), if such a periodic structure is illuminated with radiation in the stop gap, increasing power can switch it from a state with low transmissivity to a state with transmissivity of unity: the structure exhibits bistability, as first investigated by Winful *et al.*,⁶ outside the gap. This stable or multistable behavior was recently studied by Chen and Mills,^{7,8} Mills and Trullinger,⁹ and other authors¹⁰⁻¹² in terms of gap solitons. In a finite system, a gap soliton is in fact a nonlinear standing wave with a slowly varying envelope which approaches a solitonlike hyperbolic-secant shape if the periodic structure is infinitely extended.

The recent literature¹³ has focused on optical superlattices, but another way of completing and extending our

knowledge of the nonlinear properties of periodic structures is to analyze other kinds of superlattices. A periodic sequence of JTL which constitutes a one-dimensional Josephson superlattice (JSL) is an attractive system, since, as mentioned above, its basic constituent, the JTL, offers remarkable possibilities for testing various solitonic properties. Particularly, its model equation, the famous Sine-Gordon equation, may be reduced in the low-amplitude limit to the nonlinear Klein-Gordon equation and, as studied by Newell,¹⁴ coherent forms of energy can tunnel without loss to the interior of natural gap regions where the linear theory does not allow propagation. In the following we will use the term "natural gap" to characterize a gap which is inherent to the normal structure of the model equation of one JTL section, and the term "artificial gap" for gaps which result from the periodic structure of the JSL.

The aim of this paper is to present and discuss the results and novel features which emerge from our study of the nonlinear response of a JTL and a JSL in the low-amplitude limit.

There are two basic purposes of this paper. First, we present the amplitude dependence of the transmission properties in the gap of a single JTL section and then of a JSL. Second, we present the results of computer experiments on the dynamics of wave transmission through the gaps of the systems considered. The major advantages of such numerical simulations are threefold. They allow to check the calculated transmittance curves with conditions close to those of real experiments. They are useful for probing the gap-soliton characteristics, which to our knowledge have not been examined in the dynamical regime. They are of potential interest for future experiments on real superlattices.

The outline of this paper is as follows. In Sec. II we consider the transmission properties of a single JTL of finite length in the low-amplitude limit. Then the results are applied to the determination of the transmittance of a JSL. In Sec. III our theoretical results are used to calculate numerically the gap transmittance for both systems.

Then, these results are discussed and compared with those of our computer experiments on the dynamics of wave transmission through the natural gap of a JTL and the artificial gap of a JSL, which we present in the second part of this section. Section IV is devoted to concluding remarks.

II. BASIC TRANSMISSION PROPERTIES

A. Properties of a JTL section

To the lowest order of approximation, the lossless JTL may be modeled¹⁵ by the continuous electrical transmission line structure represented in Fig. 1. Here, the following quantities are defined per unit length dx : L is the inductance, C the capacitance, $I = I_0 \sin \phi$ is the Josephson tunneling supercurrent, I_0 being its maximum value, which depends on the material and the geometry of the junction. ϕ is the phase difference between the macroscopic quantum-mechanical wave functions. Applying Kirchhoff's laws to the model of Fig. 1 gives

$$\frac{\partial V}{\partial x} = -L \frac{\partial I}{\partial t}, \quad (2.1a)$$

$$\frac{\partial I}{\partial x} = -C \frac{\partial V}{\partial t} - I_0 \sin \phi, \quad (2.1b)$$

$$\frac{\partial \phi}{\partial t} = KV, \quad (2.1c)$$

where K is a constant which depends on the unit flux quantum. Introducing the transformations

$$\omega_0 t = \tau, \quad v(x, t) = V(x, t)/V_0, \quad i(x, t) = I(x, t)/I_0, \quad (2.2a)$$

with

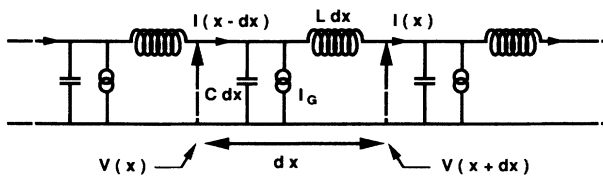
$$V_0 = \sqrt{I_0/KC}, \quad c_0^2 = 1/KLI_0, \quad \omega_0^2 = KI_0/C \quad (2.2b)$$

yields the well-known Sine-Gordon equation

$$\phi_{\tau\tau} - c_0^2 \phi_{xx} + \sin \phi = 0. \quad (2.3)$$

From Eqs. (2.1) the corresponding expressions for current and voltage along the JTL are thus given by

$$i(x, \tau) = -c_0^2 \frac{\partial \phi(x, \tau)}{\partial x}, \quad (2.4a)$$



$$\text{with: } I_G = I_0 dx \sin \phi(x)$$

FIG. 1. Equivalent continuous electrical transmission line model for the lossless Josephson transmission line (JTL).

$$v(x, \tau) = \frac{\partial \phi(x, \tau)}{\partial \tau}. \quad (2.4b)$$

In the small-amplitude limit $\phi \approx \epsilon \phi$ with $\epsilon \ll 1$, Eq. (2.3) becomes a nonlinear Klein-Gordon equation:

$$\phi_{\tau\tau} - c_0^2 \phi_{xx} + \phi - \frac{1}{6} \phi^3 = 0. \quad (2.5)$$

As is well known, Eq. (2.5) can be reduced to a nonlinear Schrödinger equation with envelope soliton solutions.^{14,16,17} Note that an equation similar to (2.5), but with different coefficients, has been recently used to investigate bistability during transmission through a linear-nondispersive–nonlinear-dispersive interface.¹⁸

Now, we use the nonlinear characteristic-matrix approach¹⁹ to calculate the transmission properties of a JTL of the finite length \mathcal{L} . Then we use the results to determine the transmittance for a combination of JTL sections, and especially for a JSL.

The solution of Eq. (2.5) for the phase may be expressed as a superposition of forward and backward propagation waves of angular frequency ω :

$$\begin{aligned} \phi(x, \tau) = & \{ \Psi^+ \exp[j(k^+ x - \omega \tau)] \\ & + \Psi^- \exp[j(-k^- x - \omega \tau)] \} + \text{c.c.}, \end{aligned} \quad (2.6)$$

where Ψ^+ and Ψ^- are, respectively, the slow-varying amplitudes of the forward and backward propagating waves; k^+ and k^- are their corresponding propagation constants; c.c. denotes the complex conjugate; and $j = \sqrt{-1}$. Substituting Eq. (2.6) in Eq. (2.5) and neglecting third harmonics, i.e., rapid terms in $e^{\pm 3j\omega\tau}$, we obtain the expressions of k^+ and k^- in the section:

$$k^+ = \frac{1}{c_0} \left[\omega^2 - 1 + \frac{|\Psi^+|^2}{2} + |\Psi^-|^2 \right]^{1/2}, \quad (2.7a)$$

$$k^- = \frac{1}{c_0} \left[\omega^2 - 1 + \frac{|\Psi^-|^2}{2} + |\Psi^+|^2 \right]^{1/2}. \quad (2.7b)$$

At this point, we remark that in the linear approximation (when one neglects $|\Psi^+|^2$ and $|\Psi^-|^2$), the wave numbers k^+ and k^- given by (2.7) are imaginary in the *natural* stop gap, i.e., when $\omega < 1$; accordingly, the waves are exponentially decaying. By contrast, from (2.7) we see that for $\omega < 1$ in the nonlinear regime (for nonzero $|\Psi^+|$ and $|\Psi^-|$) the wave numbers can remain real, and it is then possible to observe transmission in a frequency band which is forbidden in the linear regime as represented on Fig. 2.

By use of Eq. (2.6) and Eqs. (2.4a) and (2.4b), the complex amplitude of the voltage and the current at a given point x in the section may be expressed by

$$\begin{bmatrix} v \\ i \end{bmatrix}_x = \underline{M}_x \begin{bmatrix} \Psi^+ \\ \Psi^- \end{bmatrix}, \quad (2.8a)$$

where the matrix \underline{M}_x has the form

$$\underline{M}_x = -j \begin{bmatrix} \omega \exp(jk^+ x) & \omega \exp(-jk^- x) \\ c_0^2 k^+ \exp(jk^+ x) & -c_0^2 k^- \exp(-jk^- x) \end{bmatrix}. \quad (2.8b)$$

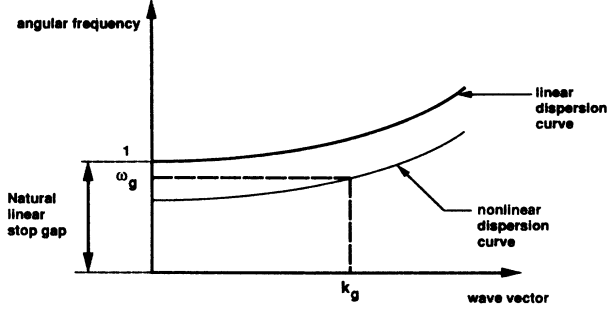


FIG. 2. Representations of the linear and nonlinear dispersion curves of the JTL: a wave with the angular frequency ω_g which lies in the natural gap ($\omega < 1$) can be transmitted if we take account of the nonlinearity.

Let us consider two points x_1 and x_2 in the JTL section. Making use of Eq. (2.8), one can express the voltage and the current at $x = x_1$ and $x = x_2$:

$$\begin{pmatrix} v \\ i \end{pmatrix}_{x=x_1} = \underline{M}_{x_1} \begin{pmatrix} \Psi^+ \\ \Psi^- \end{pmatrix}, \quad (2.9a)$$

$$\begin{pmatrix} v \\ i \end{pmatrix}_{x=x_2} = \underline{M}_{x_2} \begin{pmatrix} \Psi^+ \\ \Psi^- \end{pmatrix}, \quad (2.9b)$$

Eliminating Ψ^+ and Ψ^- from Eq. (2.9a) and Eq. (2.9b), we can relate the electrical quantities at $x = x_1$ and $x = x_2$:

$$\begin{pmatrix} v \\ i \end{pmatrix}_{x=x_2} = \underline{M} \begin{pmatrix} v \\ i \end{pmatrix}_{x=x_1}, \quad (2.10a)$$

with

$$\underline{M} = \underline{M}_{x_2} \underline{M}_{x_1}^{-1}, \quad (2.10b)$$

where \underline{M} is the characteristic matrix or transfer matrix to the JTL section of length $\mathcal{L} = x_1 - x_2$. The knowledge of this matrix \underline{M} and the boundary conditions at $x = x_1$ and $x = x_2$ allow us to characterize the transmission properties of such a section.

In order to define the transmission coefficients at the interfaces and to perform numerical simulations with conditions close to those of real experiments, each end of the JTL section is now connected, respectively, (Fig. 3) to an input linear transmission line (I) and an output linear transmission line (III). The values of L and C for these linear lines are identical to those of the JTL section (II). The characteristic velocity is thus c_0 , and the lines are nondispersive: $\omega = c_0 k_0$. In order to obtain the same expression for the voltage and the current along the whole system (I+II+III) given by Eqs. (2.4a) and (2.4b), one may define a "pseudophase" ϕ_{lin} in the linear medium:

$$\frac{\partial \phi_{\text{lin}}}{\partial \tau} = v(x, \tau), \quad (2.11)$$

with

$$\phi_{\text{lin}}(x, \tau) = (\Psi_{\text{lin}}^+ + \Psi_{\text{lin}}^-) \exp[j(k_0 x - \omega \tau)] + \text{c.c.} \quad (2.12)$$

Let us focus now on the boundary conditions at the interfaces of the JTL and the linear lines. We consider a monochromatic wave with angular frequency ω and amplitude Ψ_t transmitted in the output medium:

$$\phi_t(x, \tau) = \Psi_t \exp[j(k_0 x - \omega \tau)] + \text{c.c.} \quad (2.13)$$

The complex amplitude of the voltage and current at $x = x_1$ (output of the JTL: see Fig. 3) can be expressed in two different forms by means of Eqs. (2.4a) and (2.4b).

(i) In the linear output medium:

$$v(x_1) = -j\omega \Psi_t \exp(jk_0 x_1), \quad (2.14a)$$

$$i(x_1) = -jc_0^2 k_0 \Psi_t \exp(jk_0 x_1). \quad (2.14b)$$

(ii) In the JTL section:

$$v(x_1) = -j\omega [\Psi^+ \exp(jk^+ x_1) + \Psi^- \exp(-jk^- x_1)], \quad (2.15a)$$

$$i(x_1) = -jc_0^2 [k^+ \Psi^+ \exp(jk^+ x_1) - k^- \Psi^- \exp(-jk^- x_1)]. \quad (2.15b)$$

If we match the solution inside the JTL to the transmitted wave, we obtain the expression of the amplitude Ψ^\pm and the wave vector k^\pm of the forward and backward waves through the nonlinear section:

$$\Psi^+ = \frac{k^- + k_0}{k^+ + k^-} \Psi_t \exp[j(k_0 - k^+) x_1], \quad (2.16a)$$

$$\Psi^- = \frac{k^+ - k_0}{k^+ + k^-} \Psi_t \exp[j(k_0 + k^-) x_1], \quad (2.16b)$$

with k^+ and k^- given by Eqs. (2.7). Therefore, to have the explicit form of \underline{M} (characteristic matrix for the JTL section), one first has to solve two coupled nonlinear equations with respect to Ψ^+ and Ψ^- for a given output amplitude Ψ_t . We thus obtain the expressions of the voltage and current at $x = x_2$ (see Fig. 3). If we match the solution inside the structure to the input wave at $x = x_2$, we obtain the expression of the amplitude Ψ_{lin}^\pm of the incident and reflected wave in the linear input medium:

$$\Psi_{\text{lin}}^+ = \frac{1}{2k_0} [\Psi^+(k_0 + k^+) e^{j(k^+ - k_0)x_2} + \Psi^-(k_0 - k^-) e^{-j(k^- + k_0)x_2}], \quad (2.17a)$$

$$\Psi_{\text{lin}}^- = \frac{1}{2k_0} [\Psi^+(k_0 - k^+) e^{j(k^+ + k_0)x_2} + \Psi^-(k_0 + k^-) e^{-j(k^- - k_0)x_2}]. \quad (2.17b)$$

We then define the JTL transmittance and voltage-transfer function, given by, respectively,

$$|T|^2 = |\Psi_t / \Psi_{\text{lin}}^+|^2, \quad (\leq 1), \quad (2.18)$$

$$|T_v|^2 = |v(x_1) / v(x_2)|^2. \quad (2.19)$$

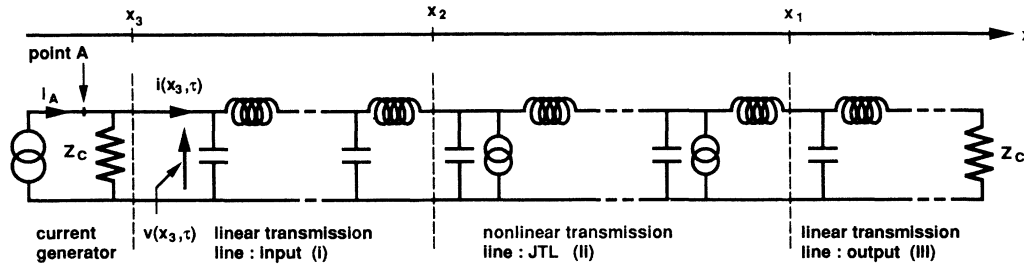


FIG. 3. Electrical model used to simulate the dynamics of waves through the JTL (II). This JTL is connected to two linear transmission lines (I) and (III) matched to their characteristic impedance Z_c .

These two basic quantities will be calculated in terms of an input parameter which will be defined in Sec. III A.

B. Properties of a JSL

One may extend the previous approach to any sequence with a number N of JTL sections (see Fig. 4) and specifically to a periodic sequence, i.e., a JSL. Both ends of this JSL are connected to the input (I) and the output (III) linear transmission line, each having the same characteristic velocity c_0 .

If the i th section has a characteristic velocity c_i and is limited by x_i and x_{i+1} , the characteristic matrix \underline{M}' for the composite system can be expressed as follows:

$$\underline{M}' = \prod_{i=1}^N \underline{M}_i(c_i), \tag{2.20}$$

where \underline{M}_i is given by Eq. (2.10), with c_0 replaced by c_i , (x_2, x_1) replaced by (x_i, x_{i-1}) , and (k^+, k^-) replaced by (k_i^+, k_i^-) . One can iterate the process presented previously for one section to calculate the set of (Ψ_i^\pm, k_i^\pm) for $i = 1, 2, \dots, N$. The knowledge of the characteristic matrix \underline{M}' yields the relations between the transmittance and incident amplitudes, i.e., the transmittance and the voltage-transfer function, which are now defined, respec-

tively, by

$$|T'|^2 = |\Psi_t / \Psi_{in}^+|^2 \quad (\leq 1), \tag{2.21a}$$

$$|T_v'|^2 = |v(x_1) / v(x_{N+1})|^2. \tag{2.21b}$$

One notices that, for a set of given values (Ψ_i^\pm, k_i^\pm) , we can numerically calculate the shape of the spatial envelope of the voltage along the x axis by use of Eq. (2.4b).

We study a specific JSL which is constituted by a sequence of JTL sections where the characteristic velocities are alternatively c_{01} and c_{02} , such that

$$c_{01}^2 = \frac{c_0^2}{1-a}, \quad c_{02}^2 = \frac{c_0^2}{1+a}. \tag{2.22}$$

Here $c_0^2 = 1/LKI_0$, and a is the modulation of the characteristic velocity c_0 . This modulation of the characteristic velocity results in an opening of forbidden frequency band or *artificial* gaps in the dispersion curve. As previously mentioned, we now use the term *artificial* to describe a gap which is due to the artificial modulation of one characteristic parameter c_0 in Eq. (2.5). In the linear approximation of this equation, the linear dispersion curve can be calculated by writing the continuity for $\phi(x, \tau)$ and its first derivative at the interface of each section. Under these conditions, one obtains²⁰

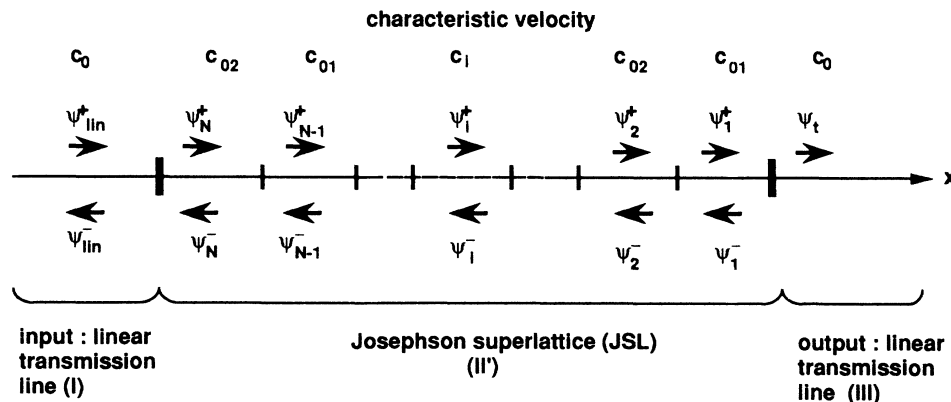


FIG. 4. Description of a JSL (II') which is built with a sequence of JTL sections with alternate characteristic velocities c_{01} and c_{02} . Each period of the superlattice consists of two alternate sections. This superlattice (II') is connected to the same linear transmission lines (I) and (III) as in Fig. 3.

$$\cos(kd) = \cos(X_1)\cos(X_2) - \frac{1}{2} \left(\frac{X_1}{X_2} + \frac{X_2}{X_1} \right) \sin(X_1)\sin(X_2), \quad (2.23)$$

with

$$X_1 = \frac{d}{2c_0} [(1+a)(\omega^2-1)]^{1/2},$$

$$X_2 = \frac{d}{2c_0} [(1-a)(\omega^2-1)]^{1/2}.$$

From the implicit linear dispersion relation (2.23), the positions of the gaps correspond to the wave vectors $k = n\pi/d$ (where d is the period of the superlattice and n is a positive integer) as represented in Fig. (5). As in the case of one single JTL section, the nonlinear effects tend to “bring down” the dispersion curve (see inset, Fig. 5). Strictly speaking, one has a nonlinear dispersion curve which is lower than the linear dispersion curve. Accordingly, if the system is excited by a sinusoidal wave with a frequency just below the upper edge of the first gap, and if the wave amplitude is increased, it can be totally transmitted through the JSL. As we shall now see in the next section, above a certain threshold, the same type of behavior, showing bistability and hysteresis, will be observed for a single JTL section and a JSL.

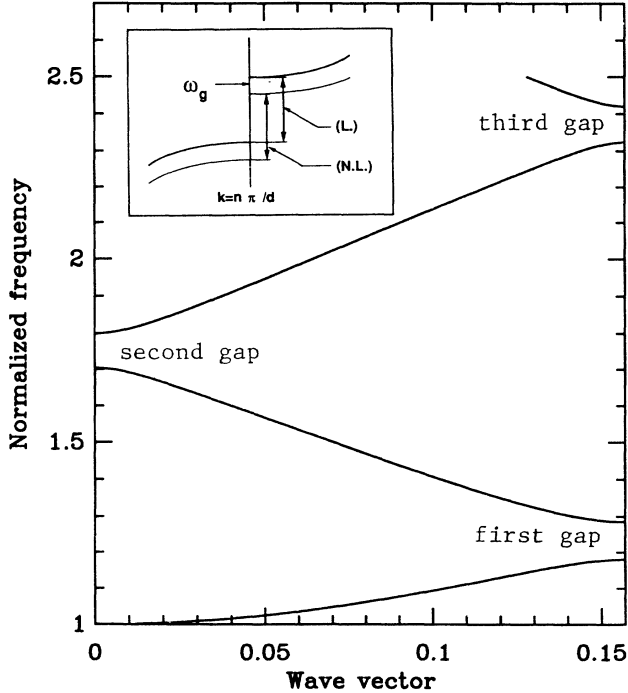


FIG. 5. Linear dispersion curve of a JSL showing the opening of stop gaps for $k = n\pi/d$ with $n=1,2,3$, $d=20$ (period of the superlattice), $c_0=4.4721$, and $a=0.4$ (modulation of the characteristic velocity c_0). Inset: details of the first gap: A wave with the angular frequency ω_g which lies in the linear artificial gap (L) can be transmitted in the nonlinear case (NL).

III. NUMERICAL STUDY AND DISCUSSION

Using the approach developed in Sec. II, we are now in position to calculate the transmittance and the voltage-transfer function for the JTL and the JSL. Then, we discuss and compare these results with those of our computer experiments on the dynamics of wave transmission in both systems, which are presented in Sec. III B and Sec. III D.

A. JTL transmission parameters

In order to calculate the transmittance, we assume that the transmitted amplitude Ψ_t at the output of the JTL section is given. By an iterative convergent method, one can calculate Ψ^\pm and k^\pm , which are given by Eqs. (2.7) and (2.16), inside the JTL section. Then, knowing these quantities in the nonlinear JTL, we calculate the amplitudes of the forward and the backward propagating waves Ψ_{lin}^\pm in the linear transmission line (I) using Eqs. (2.17). We can then find the current and the voltage at any point of the system using Eqs. (2.4), (2.6), and (2.12), and also $|T|^2$ and $|T_v|^2$. The linear transmission lines (I) and (III) are respectively matched on their characteristic impedance $Z_c=1/c_0$ in order to cancel multiple reflexions (see Fig. 3). We can now calculate the input parameter ϕ_{A0} , which is the amplitude of the pseudo-phase ϕ_A at point A:

$$\phi_A = \phi_{A0} \exp[j(k_0 x_3 - \omega \tau)] + \text{c.c.} \quad (3.1a)$$

The input current I_A is related to ϕ_A by Eq. (2.4), one obtains

$$I_A = -j c_0^2 k_0 \phi_{A0} \exp[j(k_0 x_3 - \omega \tau)] + \text{c.c.} \quad (3.1b)$$

Writing the Kirchhoff laws at $x = x_3$ yields the relation between $v(x_3, \tau)$, $i(x_3, \tau)$, and the input parameter ϕ_{A0} :

$$\phi_{A0} = \frac{|i(x_3, \tau) + v(x_3, \tau)/Z_c|}{2c_0^2 k_0}. \quad (3.2)$$

We have carried out calculations of the transmissivity of a single section of length $\mathcal{L}_1=60$ in normalized units for different angular frequencies ($\omega=0.99, 0.98$, and 0.97 in units of the natural gap frequency) in the natural linear gap, using the results obtained in Sec. II. In Figs. 6(a) and 6(b), the voltage-transfer function $|T_v|^2$ and the transmittance $|T|^2$ are plotted versus the input parameter ϕ_{A0} defined by Eq. (3.2). Both curves exhibit bistability and hysteresis. We shall now discuss in detail the case $\omega=0.99$ for $|T|^2$ in Fig. 6(b). Namely, for weak values of ϕ_{A0} , $|T|^2$ is very small (10^{-2}); if we increase ϕ_{A0} , $|T|^2$ remains practically constant until we reach a threshold (point P_1). Then the system jumps to P_2 , where $|T|^2=0.65$. If now ϕ_{A0} is decreased, $|T|^2$ continues to increase, reaches the value 1, and then decreases to point Q_2 , after which it jumps discontinuously to point Q_1 , which corresponds to a nontransmitting state. We remark (Fig. 7) that for a JTL of given length, the threshold value decreases when ω increases (in the linear gap). Moreover, as represented in Fig. 8, the threshold value decreases when the length of the JTL increases. Note

that for a length \mathcal{L} smaller than 32, the threshold notion is no more significant because a low amplitude (linear) wave can itself tunnel through the JTL section.

B. Dynamics of wave transmission through a JTL

We now present the results of our computer experiments on the dynamics of wave transmission in the natural gap of the JTL section. The conditions of our numerical simulations are close to those of a real experiment. Specifically, at the input of the electrical transmission line (I), we launch a sinusoidal wave which corresponds to the current I_A calculated previously [Eq. (3.1b)], and study its transmission through the JTL section.

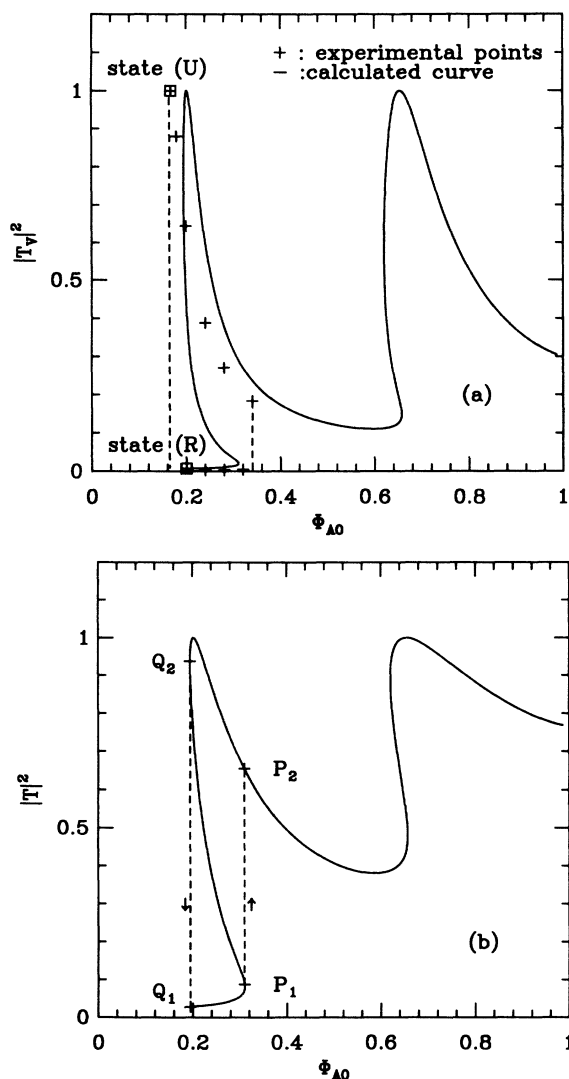


FIG. 6. Representation (a) of the voltage-transfer function $|T_v|^2$, (b) of the transmittance $|T|^2$ vs the input parameter ϕ_{A0} . The calculations are for a JTL of length $\mathcal{L}_1=60$ unit cells, characteristic velocity $c_0=4.4721$, and for an angular frequency $\omega=0.99$ in the natural gap. The states (R) and (U) correspond, respectively, to a nontransmitting and a transmitting experimental state, described in Fig. 9.

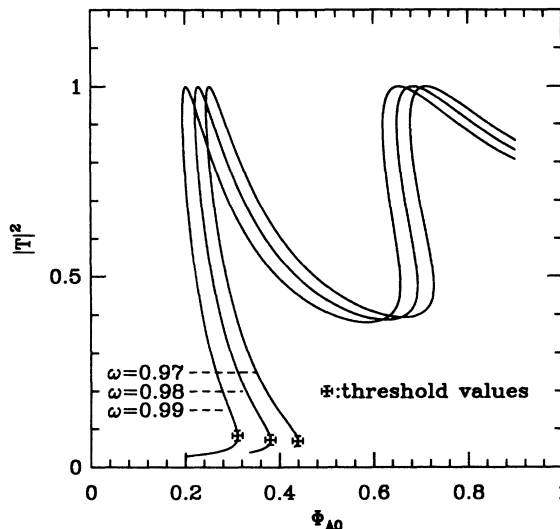


FIG. 7. Transmittance $|T|^2$ vs the input parameter ϕ_{A0} for a JTL of length $\mathcal{L}_1=60$ unit cells, characteristic velocity $c_0=4.4721$, and for three angular frequencies in the natural gap. Note the existence of a threshold value, which depends on the angular frequency ω .

The numerical simulation method is the following. Using a fourth-order Runge-Kutta method, we solve numerically the set of three coupled first-order differential equations in i, v, ϕ , obtained by writing the Kirchhoff laws at each point of the composite electrical network (I+II+III). The time step $\Delta\tau$ is chosen in order to have enough points during an oscillation (typically 80 points/oscillation). The unit length Δx , which actually

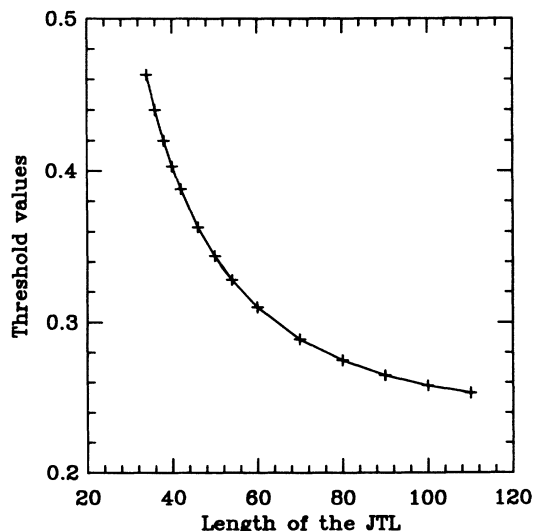


FIG. 8. Dependence of the threshold value on the length of a JTL of characteristic velocity $c_0=4.4721$, and for $\omega=0.99$.

corresponds to one electrical unit cell, is assumed to be unity. In order to avoid the numerical discretization effects, the spatial period λ must be larger than Δx ($\lambda_{\min} = 10$ unit cells).

The voltage-transfer function $|T_v|^2 = [v(x_2)/v(x_1)]^2$ is now determined by measuring the amplitudes of $v(x_1)$ and $v(x_2)$ for different values of ϕ_{A0} . The corresponding points are plotted on Fig. 6(a) and compared to the transmissivity curve previously calculated for $\omega = 0.99$. There is good agreement between the measured and calculated threshold values, but once the system has switched, one observes a slight systematic shift ($\sim 15\%$) between the measured points and the calculated curve.

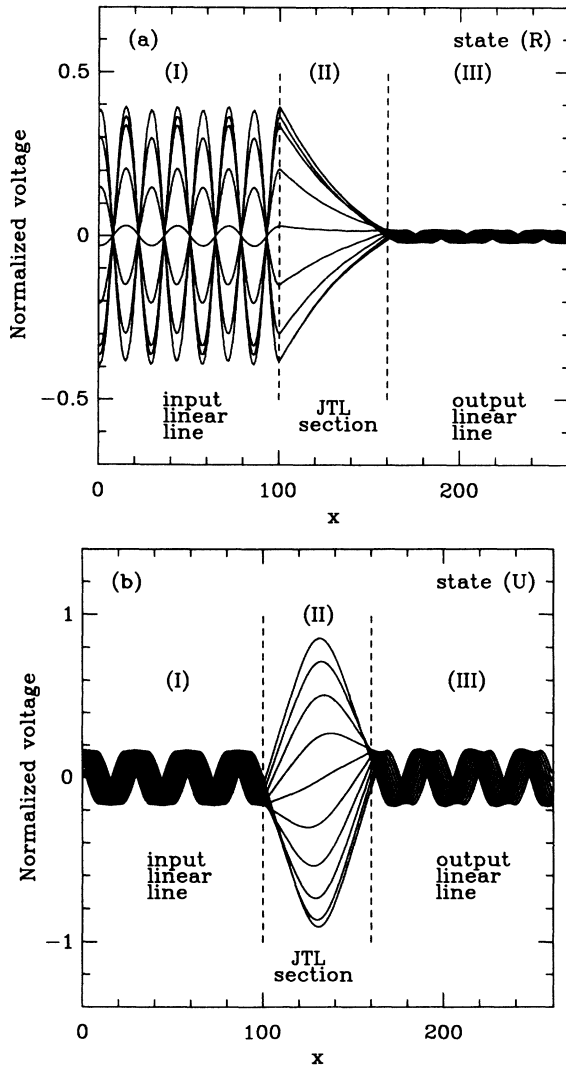


FIG. 9. Snapshots of the wave dynamics at different times in two cases: (a) the nontransmitting state with a decaying envelope in (II), (b) the transmitting state with a stationary gap soliton in (II). The system is a 60-unit cell JTL, connecting to two linear lines of length 100 unit cells, respectively matched on their characteristic impedance. The characteristics of the JTL are the same as for Fig. 6.

We attribute this shift to the fact that the low-amplitude approximation [sine expansion in (2.5)] is no longer valid inside the JTL once it has switched.

In Figs. 9(a) and 9(b), we have represented the dynamical behavior of the system, i.e., snapshots of the wave configuration at different times for $\omega = 0.99$. These figures correspond respectively to the state (R) and state (U) of Fig. 6(a). In the low-amplitude (linear) regime (state R), one observes an exponentially decreasing wave in the JTL section (II); accordingly, in the input line (I), one has a standing wave system because the incoming linear wave is practically totally reflected. In the output line (III), the transmitted wave has a very small amplitude (which corresponds to a transmittance $|T|^2 = 10^{-3}$).

In the nonlinear regime (state U), the incident wave in (I) is totally transmitted in (III); note the weak parasitic modulation, which corresponds to a slight mismatching of line (III) on the load impedance. In the JTL section (II), one has a nonlinear standing wave which looks like breathing at frequency ω . Indeed, such a breathing standing wave could be expected because it is a typical mode in the finite JTL section,^{1,14,21} which is known to oscillate at a characteristic frequency in the natural gap ($0 < \omega < 1$). It becomes the familiar breather soliton for an infinite JTL. In fact, although we have here a finite line, this stationary breather mode which appears as soon as the system has switched up to P_2 , i.e., to a similar transmitting state, may be called a gap soliton.

C. JSL transmission parameters

We now consider the JSL (II') described in Sec. II B, which contains a number N of JTL sections. The JSL is intercalated between the linear transmission lines (I) and (III). As for a single JTL section, we assume that the

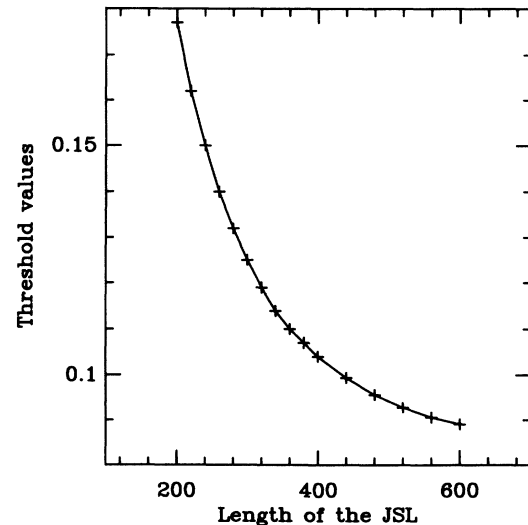


FIG. 10. Threshold values vs the length of the JSL of characteristic velocity $c_0 = 4.4721$, with modulation $a = 0.4$, period $d = 20$ unit cells, and for an angular frequency in the first artificial gap $\omega = 1.284$.

transmitted amplitude wave Ψ_t at the output is fixed. Using the method presented in Sec. III A, we calculate for the JSL the quantities Ψ_1^\pm and k_1^\pm , which correspond, respectively, to the amplitudes of the forward and the backward waves, and their corresponding wave vectors of the previous section (at the interface with the output line III). Then we iterate this process from the N th section to the first section of the JSL. Thus, we can calculate the amplitude of the forward and the backward propagating waves Ψ_{lin}^\pm in the linear transmission line (I), and also the input parameter ϕ_{A0} , which is defined in the same way as in Sec. III A). Then, calculating the coefficient $|T'|^2$ and

$|T'_v|^2$ defined by Eqs. (2.21a) and (2.21b) for different values of ϕ_{A0} , one can observe the existence of a threshold for these two quantities which depends on the length of the JSL (Fig. 10).

We have carried out calculations of the transmissivity of a JSL of period $d=20$ unit cells, modulation $a=0.4$, length $\mathcal{L}_2=16$. $d=320$ cells, and for a frequency $\omega=1.284$, which lies just below the upper edge of the first artificial gap ($k=\pi/d$). In Figs. 11(a) and 11(b), the voltage-transfer function $|T'_v|^2$ and the transmittance $|T'|^2$ are plotted versus the input parameter ϕ_{A0} defined by Eq. (3.2). As for a single JTL section, these curves exhibit bistability and hysteresis: however, the voltage-transfer function $|T'_v|^2$ as a function of ϕ_{A0} (P''_1

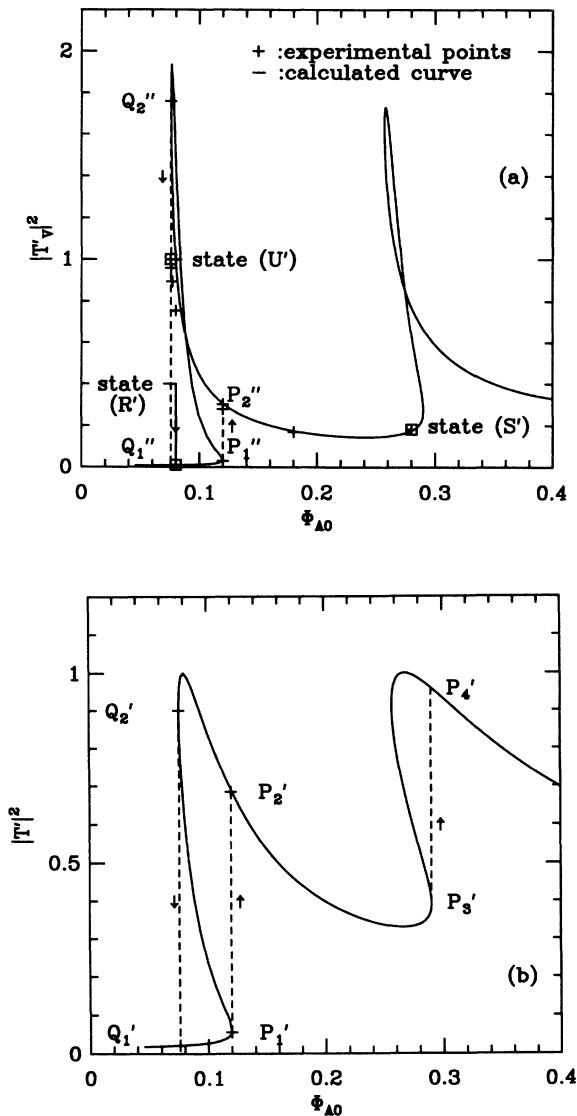


FIG. 11. Representation (a) of the voltage-transfer function $|T'_v|^2$, (b) of the transmittance $|T'|^2$ vs the input parameter ϕ_{A0} for a JSL of length $\mathcal{L}_2=16$. $d=320$ unit cells, with d the period of the JSL (20 unit cells). The characteristic velocity is $c_0=4.4721$ and the modulation $a=0.4$. The frequency lies just below the upper edge of the first artificial gap, $\omega=1.284$. The states (R') and (U') correspond, respectively, to nontransmitting and totally transmitting states.

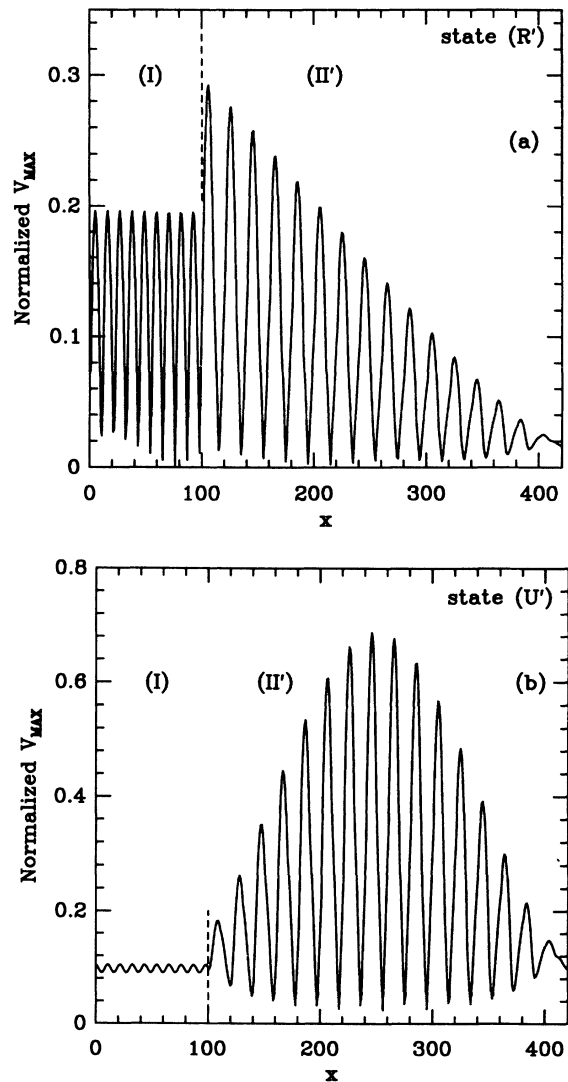


FIG. 12. Representation of the maximum voltage vs x along the linear (I) and nonlinear (II') lines: (a) for state (R') , (b) for state (U') defined in Fig. 11 and determined from our computer experiments.

$\rightarrow P_2'' \rightarrow Q_2'' \rightarrow Q_1''$) which is represented in Fig. 11(a) may be greater than unity (point Q_2''). It is due to the fact that the characteristic velocities c_{01} and c_{02} which enter in the calculations are not the same in the alternate sections of the JSL. In other terms, the voltage at the input of the nonlinear line ($x = x_2$) includes the reflected wave. We note that the system can switch down directly from Q_2'' to Q_1'' . The hysteresis cycle for $|T'|^2$ versus ϕ_{A0} ($P_1' \rightarrow P_2' \rightarrow Q_2' \rightarrow Q_1'$) in Fig. 11(b) presents a behavior similar to that presented in Fig. 6(b) for the single JTL section.

D. Dynamics of wave transmission through a JSL

We now present the results of our computer experiments on the dynamics of wave transmission in the first artificial gap of the JSL. The conditions of these experiments are the same as for the single JTL section. According to Eqs. (2.22), the JSL is realized by modulating spatially the inductances, namely, they have the values $L(1 \pm a)$. A sinusoidal wave of frequency $\omega = 1.284$ is launched at the input of the linear transmission line (I), and we measure the experimental voltage-transfer function $|T_v'|^2$ and compare these points to the transmission curve calculated in Sec. III C. We obtain better agreement between the calculated and experimental values for $|T_v'|^2$ [see Fig. 11(a)] than for the JTL section, because the range of the amplitudes is closer to the low-amplitude limit implied by Eq. (2.5).

For the sake of clarity, we have represented in Figs. 12(a) and 12(b) the spatial envelope of the voltage in each section of the JSL (for $\omega = 1.284$). In these figures, we discuss our results, which correspond, respectively, to the states (R') and (U') of Fig. 11(a). We note here that, in each section of the JSL, the combination of the forward and the backward waves (respectively, Ψ_i^+ and Ψ_i^-) gives a resonant mode. So, in order to study the transmission properties of this JSL, we have to focus on the general envelope, i.e., the envelope of each partial envelope, in the total nonlinear transmission line (II'). In the low-amplitude regime (state R'), this general envelope undergoes an exponential decay in (II'), which corresponds to a nontransmitted state ($|T_v'|^2 = 10^{-2}$). The behavior in the input (I) and output (III) line is the same as for a single JTL section: there exist a standing wave because the incoming linear wave is practically totally reflected. In the nonlinear regime (state U'), the incident wave in (I) is totally transmitted in (III), and the voltage-transfer function $|T_v'|^2$ is unity.

At this point, one must remark that in the stationary (time harmonic) regime, the model equation (2.5) may be reduced to an equation which is similar to that used by Chen and Mills⁸ in their theoretical analysis of transmission properties of optical superlattices. Namely, they described the general envelope or gap soliton in terms of Jacobi elliptic functions. Here, although we are examining a different kind of superlattice, we have verified that our numerical experiments on the wave dynamics are in good agreement with the theoretical results of Chen and Mills. Indeed, if we further increase the input parameter ϕ_{A0} , we reach state (S'), where we can see one and half

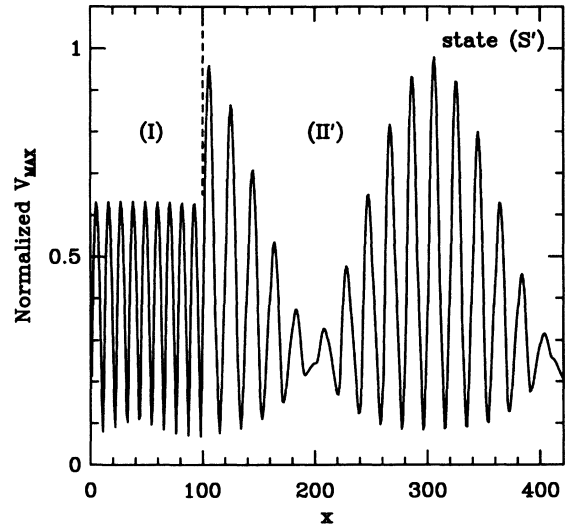


FIG. 13. Maximum voltage vs x along the system for the state (S') corresponding to Fig. 11. Note the appearance of a second period of elliptic function for the general envelope in the JSL (II').

periods of a Jacobi elliptic function, just before the system switches from point P_3' to point P_4' (see Fig. 13). Each resonant point ($|T_v'|^2 = 1$) corresponds to an integral number of periods of a Jacobi elliptic function.

As for the single JTL section, snapshots of the gap-soliton wave form at different times are represented in Fig. 14 for $\omega = 1.284$ and for the state (U') where the transmissivity is unity. The so-called gap soliton is a sta-

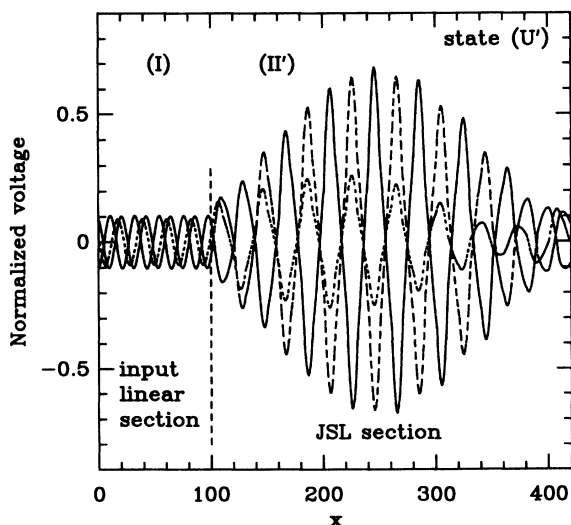


FIG. 14. Snapshots at different times of the voltage along the lines (I)+(II') showing an oscillating structure in the JSL (II'), for the state of total transmissivity (U') of Fig. 11. For the sake of clarity, we have represented the oscillating standing wave at only three different times.

tionary wave envelope which oscillates at frequency ω ; its structure looks more complicated than for the JTL case, because in each section of the JSL one has a partial standing wave.

For some experiments, after the system has switched up to the transmitting regime, modulation instability in the Benjamin-Feir sense²² may be observed (not explicitly represented here), i.e., at a given point on the JSL, instead of remaining constant, the amplitude of the voltage V_{\max} becomes unstable as time increases. In fact, Eq. (2.5) can be reduced to a nonlinear Schrödinger equation where the product of the group velocity dispersion and the non-linear term is positive. Consequently, in an infinite system, one can expect modulational instability for a plane wave: qualitatively, an amplitude-modulated wave carrier tends to break up into envelope solitons. Unfortunately, here we have a finite system with multiple reflections, and we do not know how to calculate the critical conditions for the occurrence of this instability.

Nevertheless, the modulational instability can be drastically suppressed if one adds a weak dissipation to the JSL. Namely, we have performed experiments with a conductance term G in parallel to the capacitance C in the electrical model of Fig. 1. Under these conditions, one has an additional dissipative term $g\partial\phi/\partial\tau$, where $g = GV_0/I_0$ in Eq. (2.5). To be consistent with the values of dissipation in real transmission lines,²³ we have chosen $g \sim 10^{-3}$. In Fig. 15, we have represented the spatial envelope of the waves in line (I) and JSL (II') for $\omega = 1.28$ in the gap. In this case, the modulation instability disappears, and the general behavior of the wave transmission (in the gap) is not modified, although the waves are weakly damped. Moreover, this result is important because the dissipative JSL is a more realistic model from an experimental point of view.^{5,24}

IV. CONCLUDING REMARKS

We have examined the amplitude dependence of the transmission properties in the natural gap of a JTL section and in the artificial gap of a finite JSL. We have shown that the nonlinear transmission response of both systems exhibits bistability and hysteresis and can approach unity once the amplitude of the incoming wave is greater than a certain threshold which is frequency dependent and also decreases with the length of the system. They are in good agreement with our calculations, and show that a stationary gap soliton appears as soon as the system has switched up to a transmitting state. As could be expected^{1,14} for the JTL, the gap soliton which

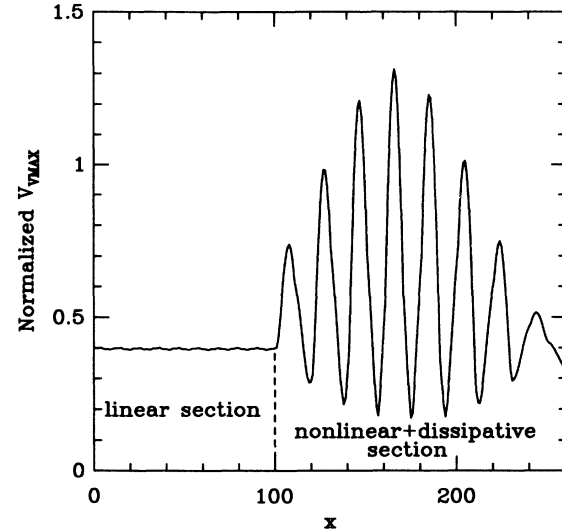


FIG. 15. Voltage envelope along the system vs x for a maximum of transmission (no reflected wave in the input linear section) determined from our computer experiments. The voltage-transfer function is less than unity because the JSL is weakly dissipative ($g = 3 \times 10^{-3}$). Its length is $\mathcal{L}_3 = 8$. $d = 160$ unit cells, with $d = 20$ unit cells (period of the JSL). The characteristic velocity is $c_0 = 4.4721$, the modulation $a = 0.4$, and the frequency $\omega = 1.28$ lies in the first artificial gap.

oscillates at a frequency in the gap behaves like a stationary breather. For the JSL, the gap soliton presents an oscillating envelope whose structure, at maximum amplitude and at a given time, agrees with the theoretical predictions.⁸

We have observed that the modulational instability in the Benjamin-Feir sense which may appear in some computer experiments is eliminated if one considers weak dissipative systems. Nevertheless, this phenomenon should be considered carefully in future investigations of the nonlinear response in the gaps of real physical systems.

Our computer experiments of the wave dynamics show how the systems would behave in practice. This suggests the gap-soliton-mediated bistability should be observed experimentally on a real JTL and JSL. The experimentalist should be able to realize practically the JSL by modulating the inductance (per unit length), which depends simply on the geometrical parameters of a superconducting line.

¹R. D. Parmentier, in *Solitons in Action*, edited by K. Lonngreen and A. C. Scott (Academic, New York, 1978).

²A. Barone and G. Paterno, *Physics and Application of the Josephson Effect* (Wiley, New York, 1982).

³K. K. Likharev, *Dynamics of Josephson Junctions and Circuits* (Gordon and Breach, New York, 1986).

⁴P. S. Lomdahl, *J. Stat. Phys.* **39**, 551 (1985).

⁵N. F. Pedersen, in *Superconducting Electronics*, Vol. 59 of *NATO Advanced Study Institute Series F: Computer and System Sciences*, edited by H. Wienstock and N. Nisenoff (Springer-Verlag, Berlin, 1989), p. 209.

⁶H. G. Winful, J. H. Marburger, and E. Garmire, *Appl. Phys. Lett.* **35**, 379 (1979).

⁷W. Chen and D. L. Mills, *Phys. Rev. Lett.* **58**, 160 (1987).

- ⁸W. Chen and D. L. Mills, *Phys. Rev. B* **36**, 6269 (1987).
⁹D. Mills and S. E. Trullinger, *Phys. Rev. B* **36**, 947 (1987).
¹⁰J. E. Sipe and H. G. Winful, *Opt. Lett.* **13**, 132 (1988).
¹¹C. Martijn de Sterke and J. E. Sipe, *Phys. Rev. B* **38**, 5149 (1988).
¹²J. Coste and J. Peyraud, *Phys. Rev. B* **40**, 12 201 (1989).
¹³D. N. Christodoulides and R. I. Joseph, *Phys. Rev. Lett.* **62**, 1746 (1989).
¹⁴A. C. Newell, *J. Math. Phys. (New York)* **19**, 1126 (1978).
¹⁵J. C. Swihart, *J. Appl. Phys.* **32**, 461 (1961).
¹⁶G. L. Lamb, *Elements of Soliton Theory* (Wiley, New York, 1980).
¹⁷M. Remoissenet, *Phys. Rev. B* **33**, 2386 (1986).
¹⁸G. Cao and P. P. Banerjee, *J. Opt. Soc. Am. B* **6**, 191 (1989).
¹⁹S. Dutta Gupta and D. S. Agarwal, *J. Opt. Soc. Am. B* **4**, 691 (1987).
²⁰L. Brillouin, *Wave Propagation in Periodic Structures* (Dover, New York, 1953).
²¹R. M. DeLeonardis and S. E. Trullinger, *J. Appl. Phys.* **51**, 1211 (1980).
²²T. B. Benjamin and J. F. Feir, *J. Fluid Mech.* **27**, 417 (1967).
²³A. C. Scott, F. Y. F. Chu, and S. A. Reible, *J. Appl. Phys.* **47**, 3272 (1976).
²⁴A. Fujimaki, K. Nakajima, and Y. Sawada, *Phys. Rev. Lett.* **59**, 2895 (1987).